Accelerator Department
BROOKHAVEN NATIONAL LABORATORY
Associated Universities, Inc.
Upton, New York 11973

AGS DIVISION TECHNICAL NOTE

No. 133

STUDIES OF SLOW BEAM EXTRACTION WITH AND WITHOUT AN ELECTROSTATIC SEPTUM

J.W. Glenn and H. Weisberg
May 6, 1977

We calibrated the secondary emission chamber and loss monitor which are used to measure the Slow Extracted Beam extraction efficiency. Using these monitors, we measured (and changed) the spiral pitch, we measured the effective thickness of the F5 magnetic septum and the H20 electrostatic septum, and we measured the extraction efficiency with and without the H20 septum. In addition, we studied vertical losses at the F10 ejector. The H20 septum made a significant improvement, but starting from a level that is considerably worse than it should be. Many areas for improvement are suggested.

I. Introduction

Slow extraction[1] of the AGS beam is normally done in two stages, using septum magnets at F5 and F10 (see Table 1). To improve the extraction efficiency, an electrostatic septum deflector (see Table 1) has been installed at H20,[2] but has never been used for normal operation. In February we studied various aspects of the slow beam extraction with and without the H20 device. The results of these studies, which raise as many questions as they answer, are presented here.

II. Secondary Emission Chamber Aging Effects

We scanned the beam horizontally across the secondary emission chamber[3] that is located at the beginning of the SEB line (CE10) and across the one just upstream of the B target. Figures 1 and 2 give the response vs. position for these devices, and show the well-known effect of aging; the response at the place where the beam normally passes is low by $\sim$ 15%. This aging effect makes systematic studies of beam extraction difficult since the

SEC response is a function not only of beam intensity but also of steering and of integrated exposure to protons.

Several cures for this problem are being investigated.[4]

III. Loss Monitor Response

Loss monitors[5] are installed in various places (Fig. 3) to monitor the slow beam extraction. One change which we made was to read separately the F5+F7 and the F10 monitors; we could then study the separate losses on the F5 and F10 magnets.

The loss monitor response was studied by inducing beam losses at various points along the ring. Figure 4 shows the response of the ring loss monitor to losses induced by varying the F5 septum magnet current and the ring sextupole current. Here CBM is the readout of the circulating beam toroid which has a calibration of 100 counts per 10^{12} protons. The losses induced by the two different methods lie on the same straight line. The intercept of this line on the horizontal axis at 8.0 is a measure of the relative response of the C10 SEC and the circulating beam toroid and, assuming the latter is accurate, shows that the former has a calibration of 800 counts per 10^{12} protons. The SEC integrator gain had been set initially by foil activation with an unaged chamber to give 1000 counts/10^{12}; the reduction to 800/10^{12} is presumably related to the aging effect described in the previous section.

The intercept of the line in Fig. 4 with the vertical axis at 6.0, or equivalently the slope of -0.75, gives a RLM calibration for beam loss of 600 counts/10^{12} protons. This calibration will obviously depend on where in the ring the protons are lost, and on the details of how they are lost and how much material is nearby to shield or to make cascades. We studied this variation for a number of sources of loss. In each case the range of loss was much smaller than was the case for the data of Fig. 4, so the calibration was by slope rather than intercept.

Calibration curves thus obtained for various sources of loss are shown in Figs. 4-9 for RLM, in Figs. 10-13 for F10LM, in Figs. 14-15 for F5LM and in Figs. 16-17 for H20LM. Clearly the losses for a given monitor do not lie on a universal straight line. In fact, even for loss generated in a particular way (for example, in Fig. 4 by varying

the F10 radius) the loss points tend to lie on a curve with two branches, one corresponding to radius less than optimum, the other to radius greater than optimum. Away from the minimum, however, the points in a given branch tend to lie on straight lines and we can assign slopes and hence calibration factors. These factors are summarized in Table 2.

Losses were also induced by flipping the J19 target and by adjusting the spill servo to give a spike at the end of the spill; loss monitor responses for these losses are also given in Table 2.

The RLM response factors obtained in this way lie in a fairly narrow range for all the sources of loss tried, except for the J19 target loss. In particular, the response is similar for losses on each of the three extraction septa, simulating losses during normal extraction. Based on the measured responses, we assign universal calibration factors for each of the four loss monitors given in the last line of Table 2. From the variation of the measured responses, we assign somewhat arbitrarily an error of ± 30% to each calibration factor.

The F10 loss monitor responds to losses on both the F5 and F10 septa. The individual losses at F5 and F10 can be obtained from the F5 and F10 loss monitor signals by inversion. We have

$$(\text{F5LM/CBM}) = (\text{loss on F5 septum}) \cdot (100/100)$$

$$(\text{F10LM/CBM}) = (\text{loss on F5 septum}) \cdot (40/100) + (\text{loss on F10 septum}) \cdot (120/100)$$

and therefore,

$$\text{loss on F5 septum} = (\text{F5LM/CBM}) \cdot (100/100)$$

$$\text{loss on F10 septum} = (\text{F10LM/CBM}) \cdot (100/120) - (\text{F5LM/CBM}) \cdot (100/100) \cdot (40/120)$$

The other losses are given by:

$$\text{loss on H20 septum} = (\text{H20LM/CBM}) \cdot (100/10000)$$

$$\text{total ring loss} = (\text{RLM/CBM}) \cdot (100/620)$$

IV. Spiral Pitch

Figure 18 shows the variation in ring loss and H20 loss as the H20 septum radial position in changed. These measurements were made with recent operational settings of the slow beam parameters. The spiral pitch at H20 can be read from this graph as the distance between the dip in ring loss near 1.8 inches (where the H20 septum shadows the F5 septum) and the fall-off in H20 loss near 2.2 inches (where the septum has moved to the edge of the extracted beam). The spiral pitch or beam width thus obtained is 0.42 inches. Since the horizontal aperture of the H20 device is only 0.39 inches, there is a precipitous rise in H20 loss near the normal operating position of 1.8 inches. Using the F5 flag, we measured the spiral pitch at F5 and found a value of 0.8 ± 0.05 inches. The spiral pitch at F5 is greater than that at H20 both because F5 is a horizontal beta maximum and because the beam spirals almost three turns in going from H20 to F5 and hence the spiral pitch grows. The measured ratio of spiral pitches is 1.9.

In order to clear the H20 horizontal aperture, we reduced the F5 and H20 orbit bump currents and thereby reduced the spiral pitch to a value, measured on the F5 flag, of 0.6 ± 0.05 inches. We then obtained the H20 radial scan results in Fig. 19, showing a spiral pitch at H20 of 0.29 inches and no sharp rise of H20 loss at small radius.

Figure 19 also gives us a measurement of the horizontal variation of beam density (as the beam spirals out its density decreases). If we define

$$f = \frac{\text{beam density at nominal septum radial position}}{\text{average beam density}}$$

then the H20 loss curve in Fig. 19 gives f = 1.5. This factor f is important in estimating beam loss at septa. If t is the effective septum thickness (including beam divergence effects) and s is the spiral pitch, then the expected beam loss is

$$L = \frac{ft}{s}$$

V. Effective Septum Thicknesses

Figure 20 gives the measured F5 loss vs. F5 skew angle. This curve is much broader than expected for a 0.030 inch septum, and its minimum loss value, L = 0.17, is much greater than expected. It implies an effective septum thickness of 0.090 inches.

We later examined the copper septum and found large bumps on it near its leading edge. The magnet was too radioactive to justify a mechanical measurement of the thickness of these bumps.

Figure 21 is the corresponding skew curve for the H20 electrostatic septum. Here also the minimum loss value is much greater than expected; the value L = 0.073 at 83 kV corresponds to an effective thickness of 0.014 in. Since the expected contribution of beam divergence is only 0.002 in., there is a considerable discrepancy. Another feature of the H20 loss was that it varied with time, by as much as a factor of two over a period of several days. It is conjectured that foil wrinkling related to beam heating of the foil and of the solid steel cathode is an important effect. Tests of this idea are planned.

VI. Vertical Losses at F10

With the separate readout of F5 and F10 losses, we found that there was a beam loss of several percent on the F10 ejector magnet. There were several indications that this loss came from vertical aperture scraping: (1) the beam spot on the F10 flag was off-center vertically; (2) when we scraped the beam with the J10 vertical target, the F10 loss decreased while the F5 loss stayed the same; (3) we steered the beam vertically with the F20 and I15 vertical bump magnets and found that the F10 loss could be reduced. Unfortunately, there is also another vertical loss problem, at the A/C splitter AD019, and since F20 and I15 are the same phase we could not steer for simultaneous clearance at both apertures. The I15 vertical bump magnet will be moved to I10 to improve this situation.

VII. Extraction Efficiency With and Without the Electrostatic Septum

Figure 22 shows the F5 loss vs. F5 septum radial position, for various voltages on the H20 septum. Even with no applied voltage, there is a loss reduction when the septum shadows are lined up.[6] As the high voltage increases, the valley in the curve gets wider and deeper. From the curves we can infer a deflection at F5 of about 0.3 inches for each milliradian of bend at H20. Since H20 is almost

References and Footnotes

1. L. Blumberg, M.Q. Barton, G.W. Bennett, J.D. Fox, J.W. Glenn, H.C.H. Hsieh, R.J. Nawrocky and A.V. Soukas, Proceedings of the 1969 Particle Accelerator Conference, Washington, D.C.

2. J.W. Glenn, AGS Division Internal Report 69-5 (1969).

3. R.L. Witkover, AGS Division Internal Report 76-1 (1976).

4. E.L. Garwin and N. Dean, Proceedings of the Conference on Beam Intensity Measurement, Daresbury, 1968.

5. F. Hornstra, L. Blumberg, J.W. Glenn, J. Keane, Y.Y. Lee, L. Smith and A. Soukas, AGS Technical Note No. 112 (1974).

6. A. Maschke, FN-100, Fermilab 1967.

Distr: Accel. Dept. S&P

exactly an integral number of wavelengths (24) upstream of F5 at the extraction tune of 8 2/3, this deflection would be zero in the absence of non-linear effects. The deflection comes about because of the non-linear growth of radius in resonant extraction. The calculated value[2] is 0.34 inches.

Table 3 gives a comparison of the extraction efficiency with and without H20. In the process of turning on H20, we also changed the spiral pitch at F5 from 0.8 to 0.6 inches. Presumably the extraction efficiency without H20 but with 0.6 inches spiral pitch would have been even worse than shown.

With 0.8 inch spiral pitch, the horizontal emittance of the extracted beam is much larger than had been assumed in designing the switchyard. Indeed, there was a dramatic improvement in the switchyard efficiency with reduced spiral pitch, as shown in the next to last line in Table 3. The net result that the overall ratio of delivered beam to circulating beam improved from 52% to 70%.

About two shifts of operation under these improved conditions were accumulated before the shutdown time arrived.

Table 1

Slow Beam Extraction Devices

Location	Length	Excitation	Field	Deflection	Septum Thickness	Aperture (in.) Horiz.	Aperture (in.) Vert.
H20	60 in.	80 kV	80 kV/cm	0.43 mrad	0.003 in.	0.39 in.	
F5	26 in.	2100 A	1.5 kG	1.1 mrad	0.030 in.	1.25 in.	0.687 in.[a]
F10	32+48 in.	4800 A	9.5 kG	20 mrad	0.53 in.	1.5 in.	0.75 in.

[a] 0.56 in. clearance between cooling tubes

Table 2

Loss Monitor Responses to Various Loss Sources

Parameter Varied	Response, counts per 10^{12} protons lost RLM	F10LM	F5LM	H20LM
F5 septum current	600			
Sextupole current	600			
F10 radius	620-640	120		
F10 skew	350-630	125		
F5 radius	650	45	120	
F5 skew	360-520	30	80	
H20 radius				7400
H20 skew	580			14000
J19 vertical target	100			
Spike at end of spill	610			
Old calibration factor	620	160[a]	160[a]	30000
New value adopted	620	120[b] 40[c]	100	10000

[a] F10LM and F5LM had been added electronically

[b] reponse to losses at F10

[c] response to losses at F5

Table 3

Performance With and Without the H20 Septum

H20 Septum	Retracted	83 kV/cm
Spiral pitch at F5	0.8 in.	0.6 in.
H20 loss	0.00	0.07
F5 loss	0.17	0.04
F10 loss	0.025	0.02
Ring loss	0.21	0.13
Extraction efficiency: CE10/CBM (corrected)	0.78	0.85
Switchyard efficiency: A+B+C/CE10	0.67	0.82
Total SEB efficiency: A+B+C/CBM	0.52	0.70

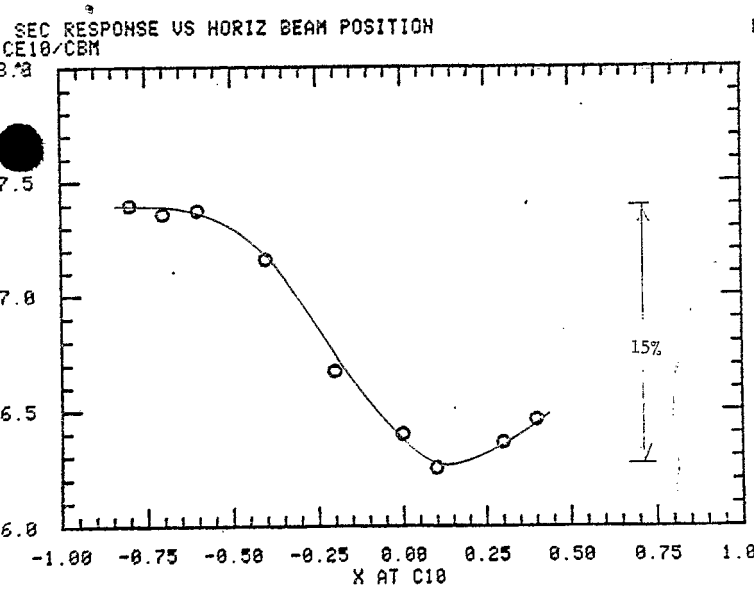

Fig. 1 Response of the C10 secondary emission chamber as the horizontal beam position is varied. The horizontal position is given in inches.

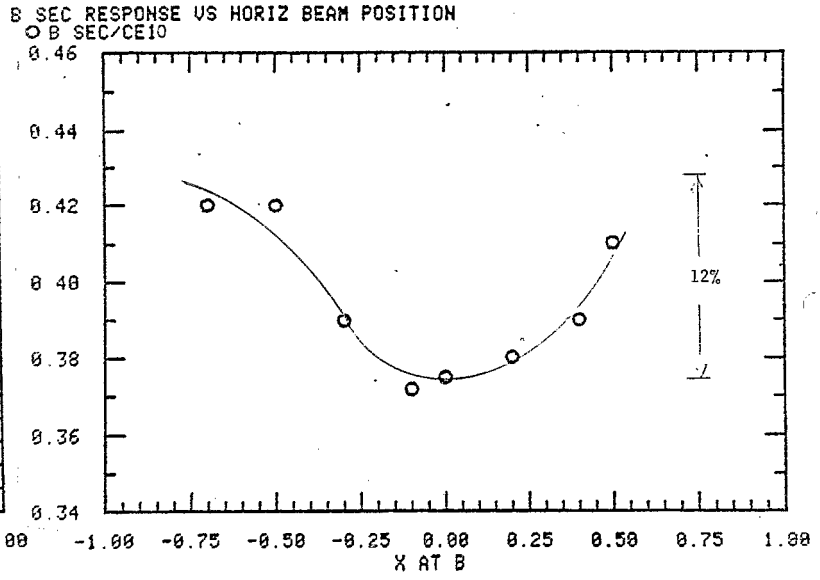

Fig. 2 Response of the B secondary emission chamber as the horizontal beam position is varied. The horizontal position is given in arbitrary units.

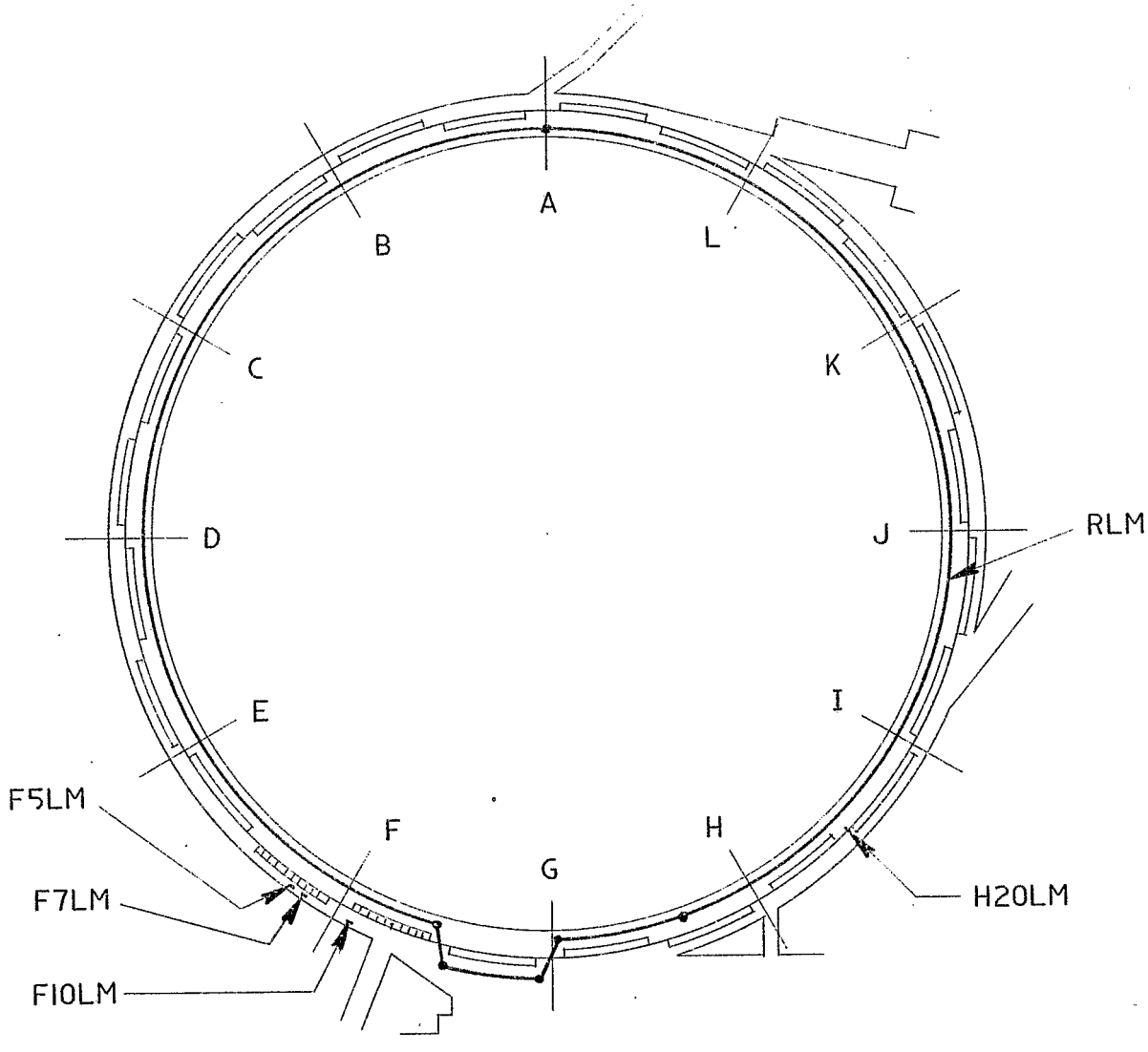

Fig. 3 Location of the slow extraction loss monitors. The monitors at F5 and F7 are added electronically and read out as F5LM; the others are read individually.

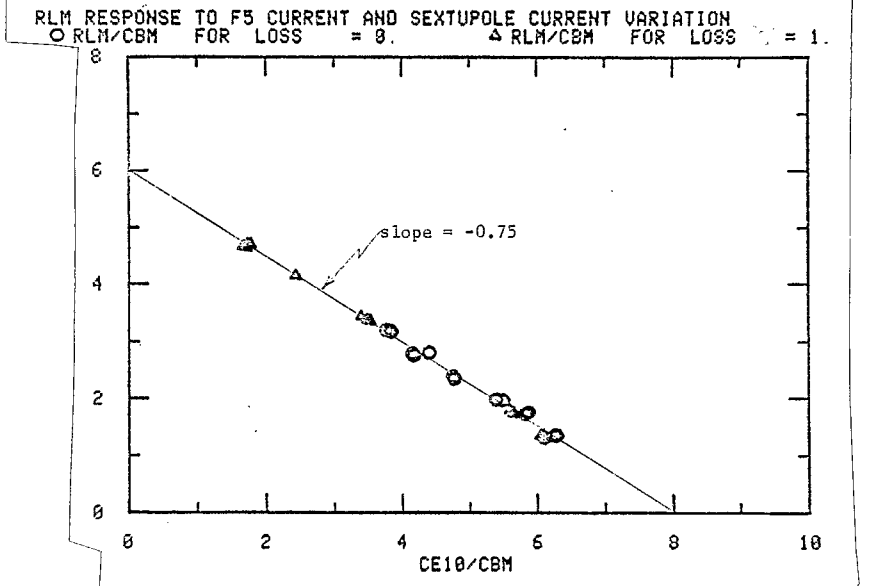

Fig. 4 Response of the ring loss monitor to losses induced by varying the F5 septum magnet current (circles) and the ring sextupole current (triangles).

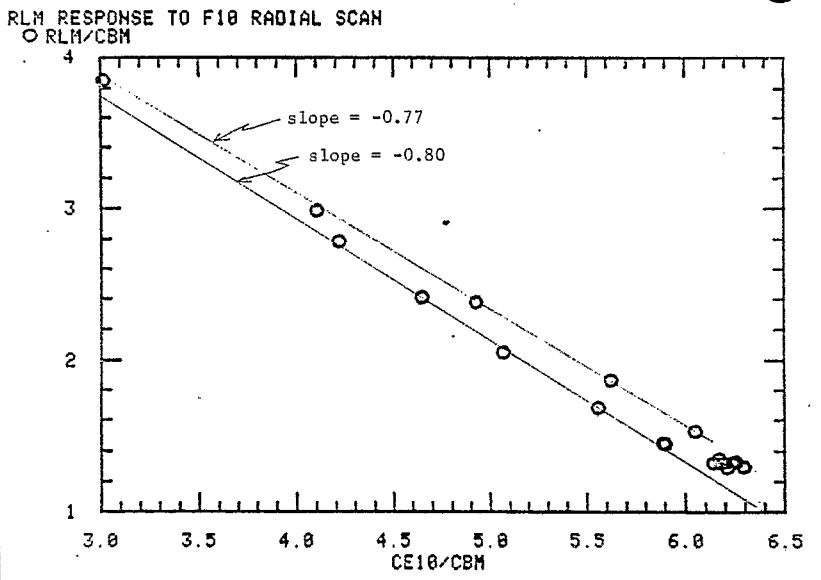

Fig. 5 Response of the ring loss monitor to losses induced by varying the F10 septum magnet radial position.

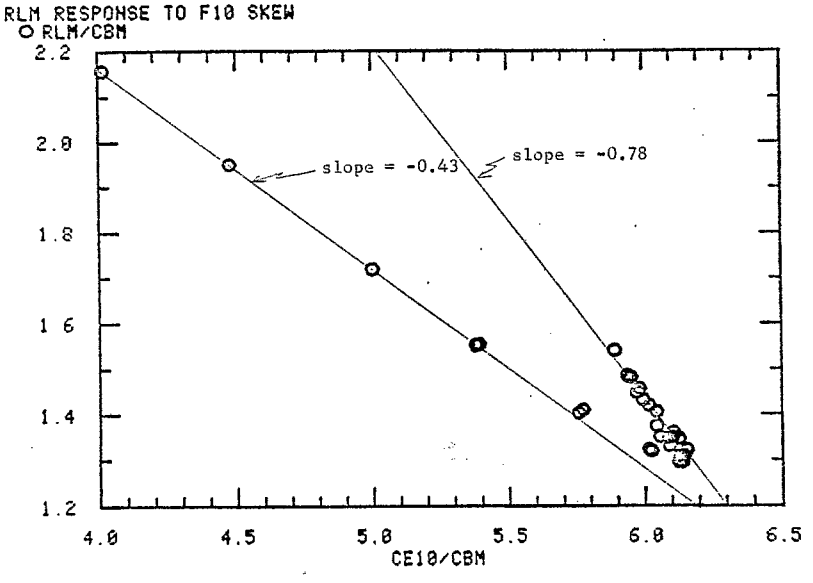

Fig. 6 Response of the ring loss monitor to losses induced by varying the F10 septum magnet skew angle.

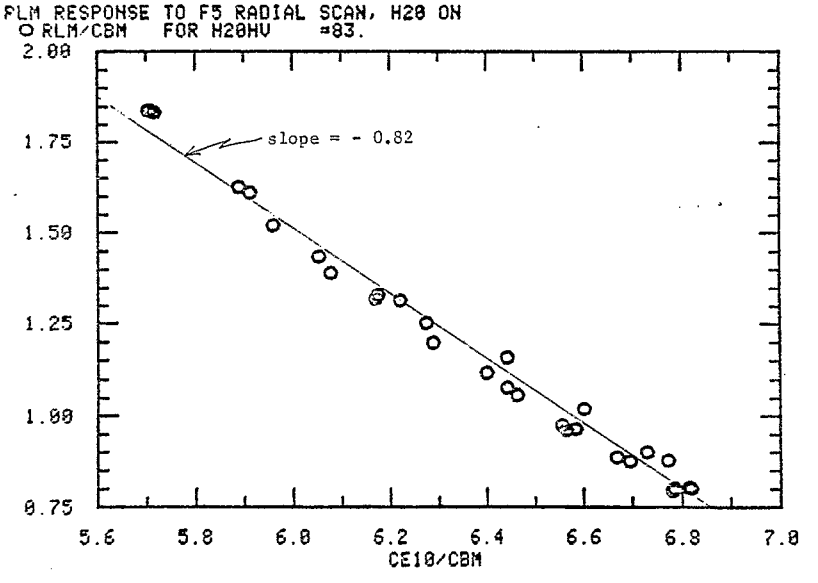

Fig. 7 Response of the ring loss monitor to losses induced by varying the F5 septum magnet radial position.

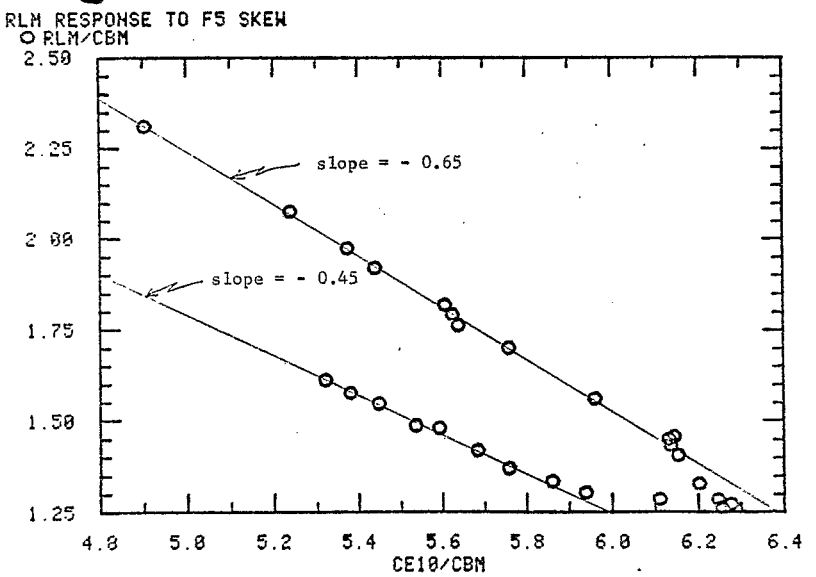

Fig. 8 Response of the ring loss monitor to losses induced by varying the F5 septum magnet skew angle.

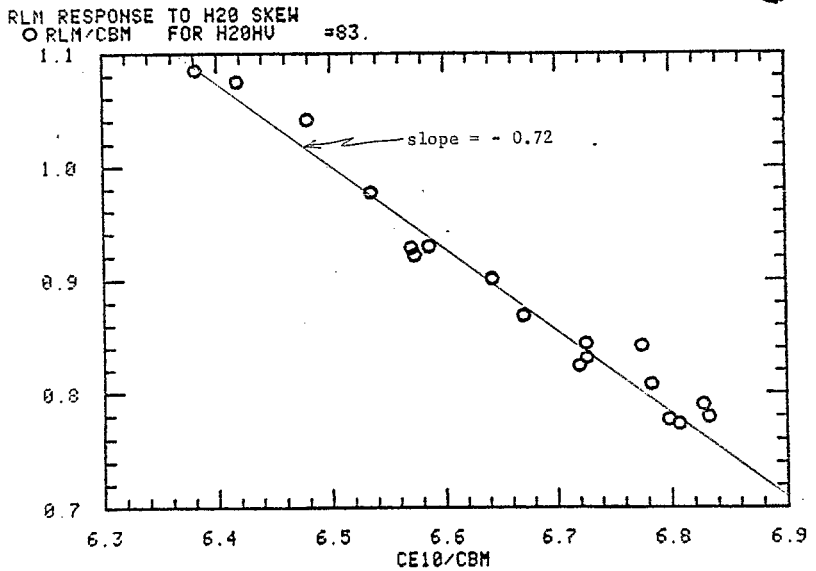

Fig. 9 Response of the ring loss monitor to losses induced by varying the H20 electrostatic septum skew angle.

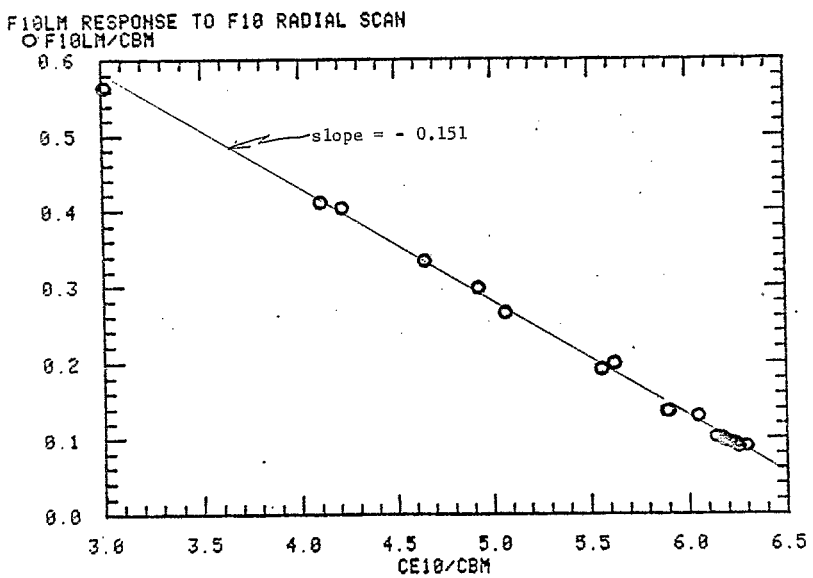

Fig. 10 Response of the F10 loss monitor to losses induced by varying the F10 septum magnet radial position.

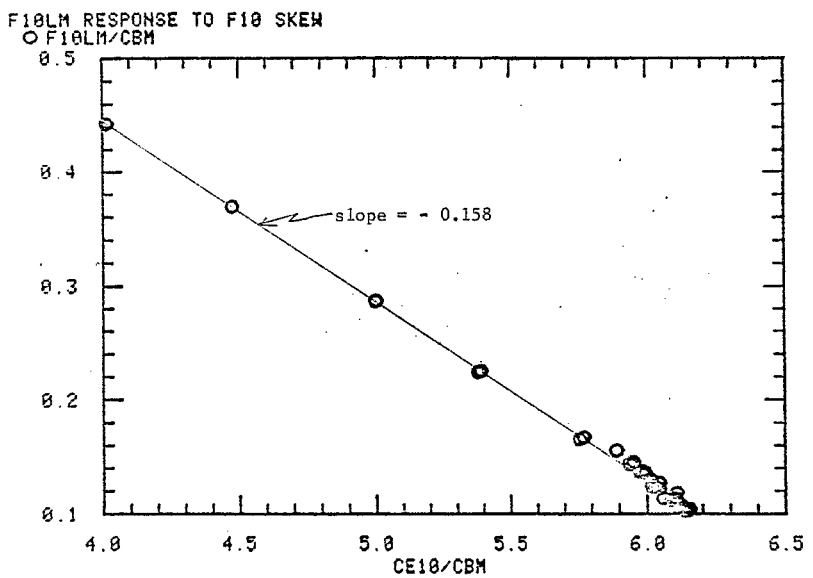

Fig. 11 Response of the F10 loss monitor to losses induced by varying the F10 septum magnet skew.

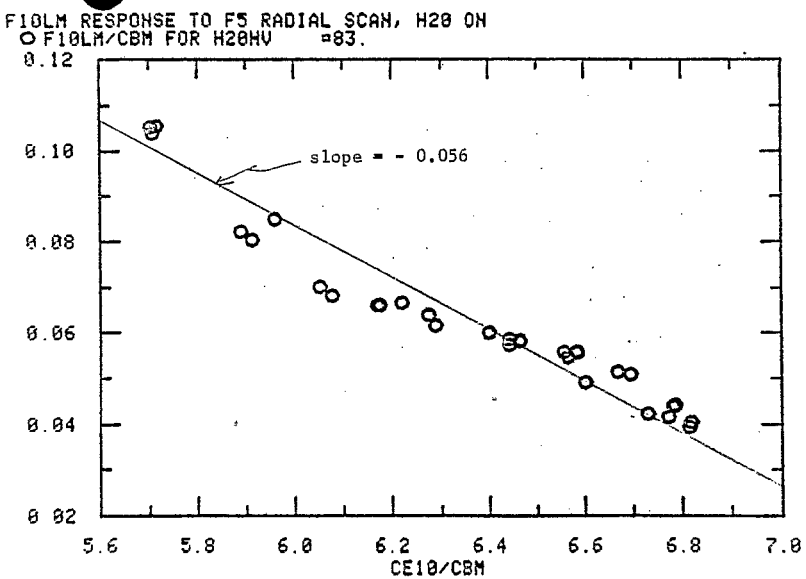

Fig. 12 Response of the F10 loss monitor to losses induced by varying the F5 septum magnet radial position.

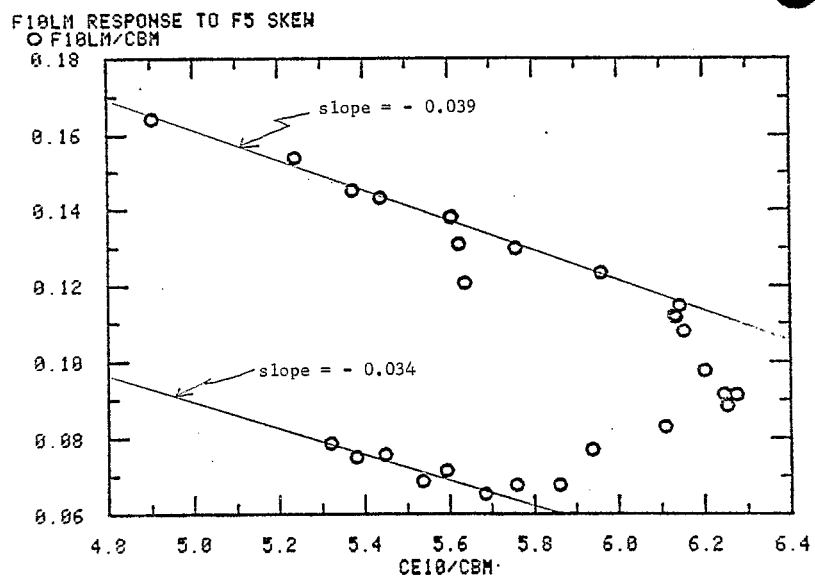

Fig. 13 Response of the F10 loss monitor to losses induced by varying the F5 septum magnet skew angle.

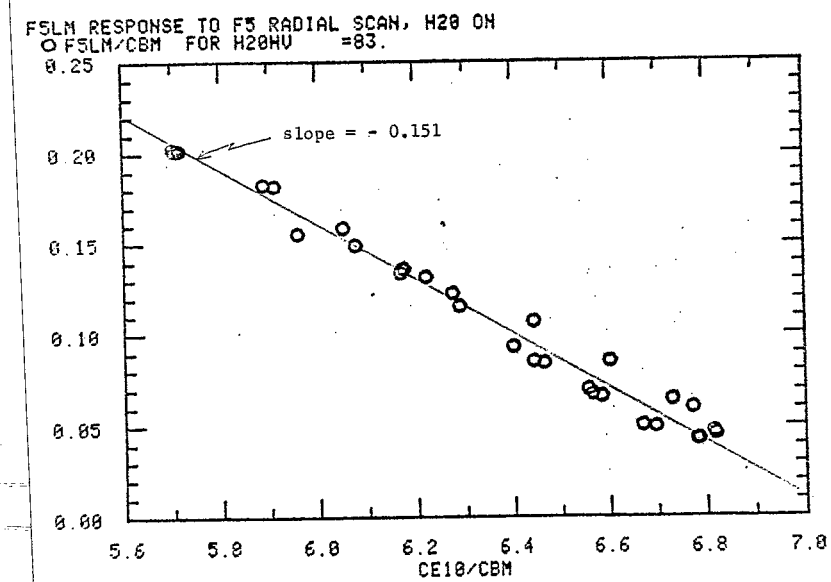

Fig. 14 Response of the F5 loss monitor to losses induced by varying the F5 septum magnet radial position.

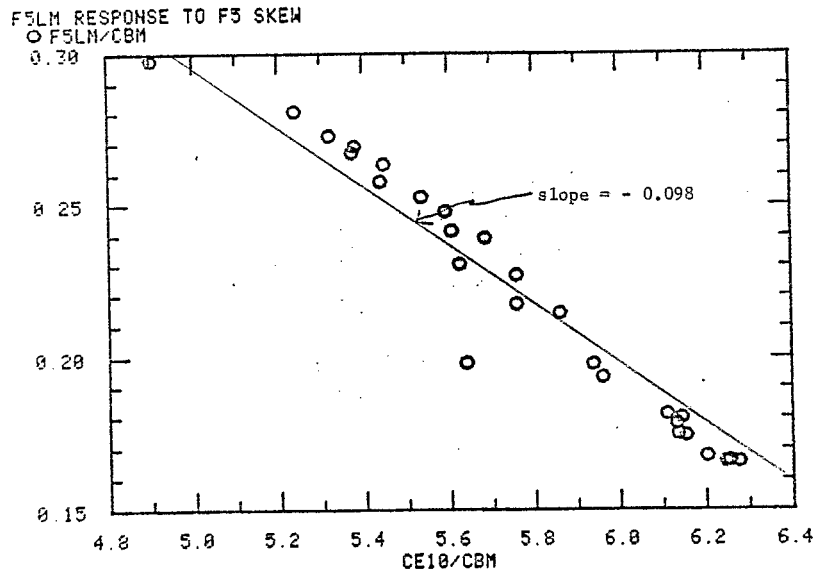

Fig. 15 Response of the F5 loss monitor to losses induced by varying the F5 septum magnet skew angle.

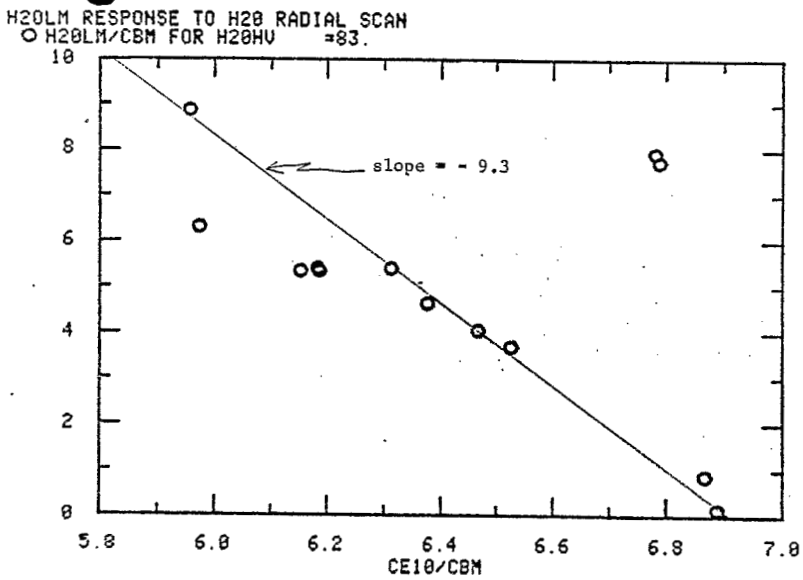

Fig. 16 Response of the H20 loss monitor to losses induced by varying the H20 electrostatic septum radial position.

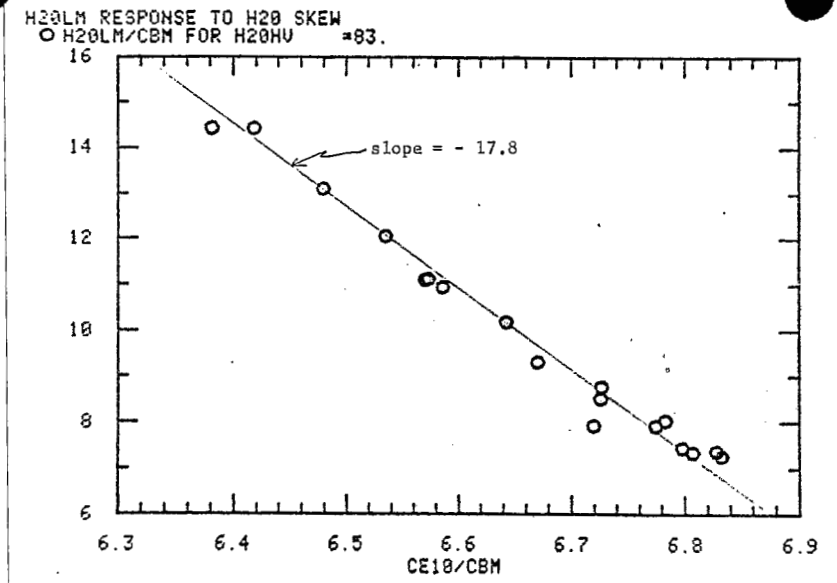

Fig. 17 Response of the H20 loss monitor to losses induced by varying the H20 electrostatic septum skew angle.

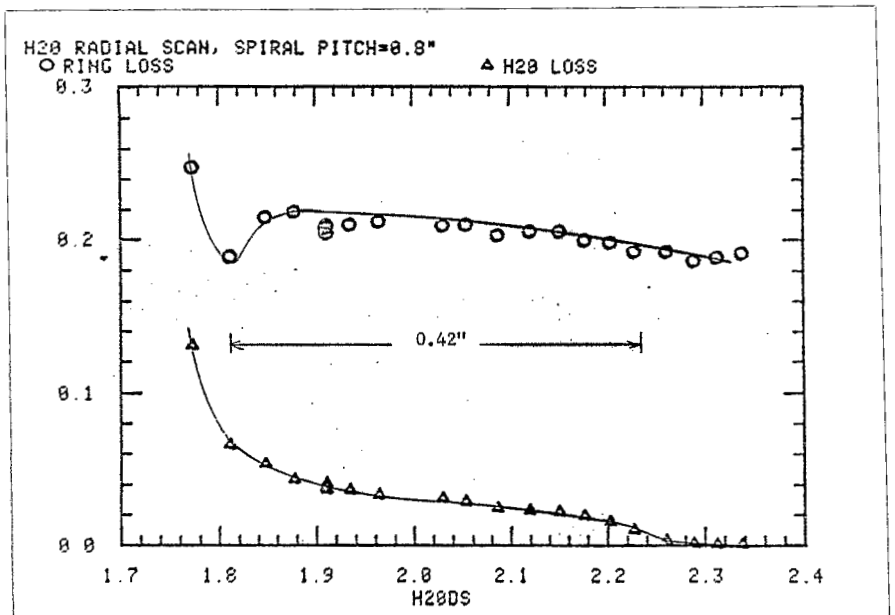

Fig. 18 Ring loss and H20 loss vs H20 downstream radial position in inches. The upstream position was adjusted at each point to minimize the H20 loss. The H20 high voltage was off. Measurements were made with a spiral pitch measured on the F5 flag of 0.8 ± 0.05 inches.

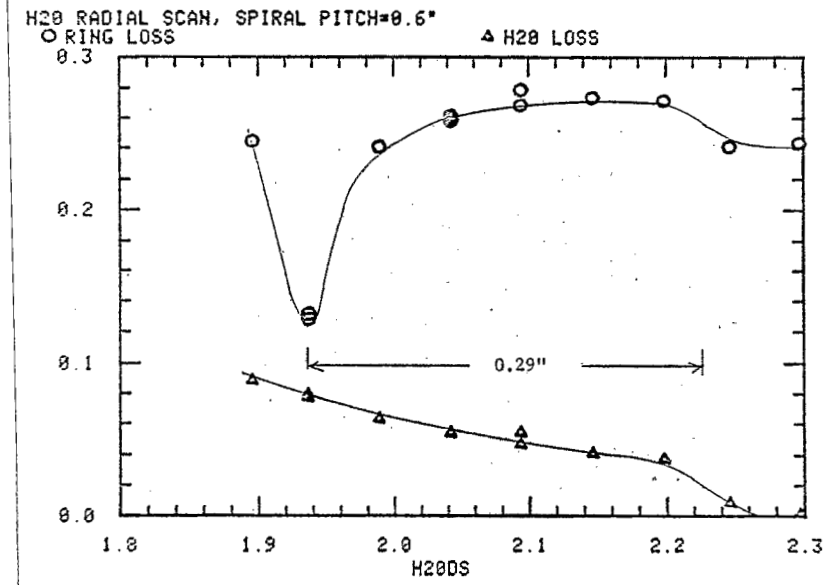

Fig. 19 Ring loss and H20 loss vs H20 downstream radial position in inches. The upstream position was adjusted at each point to minimize the H20 loss. The H20 high voltage was 83 kV. Measurements were made with a spiral pitch measured on the F5 flag of 0.60 ±0.05 inches.

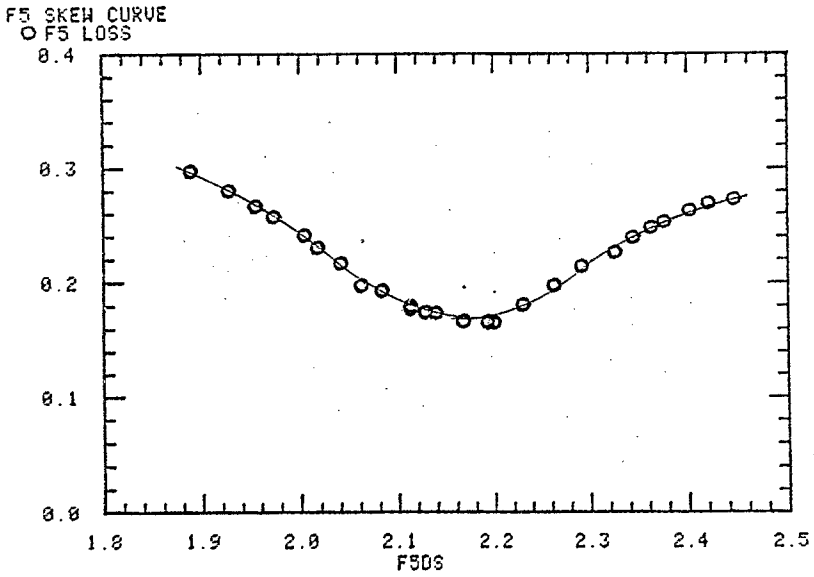

Fig. 20 Beam loss at F5 vs F5 septum downstream position in inches. The upstream position was held fixed. Measurements were made with the H20 electrostatic septum retracted, and with a spiral pitch at F5 of 0.8 inches.

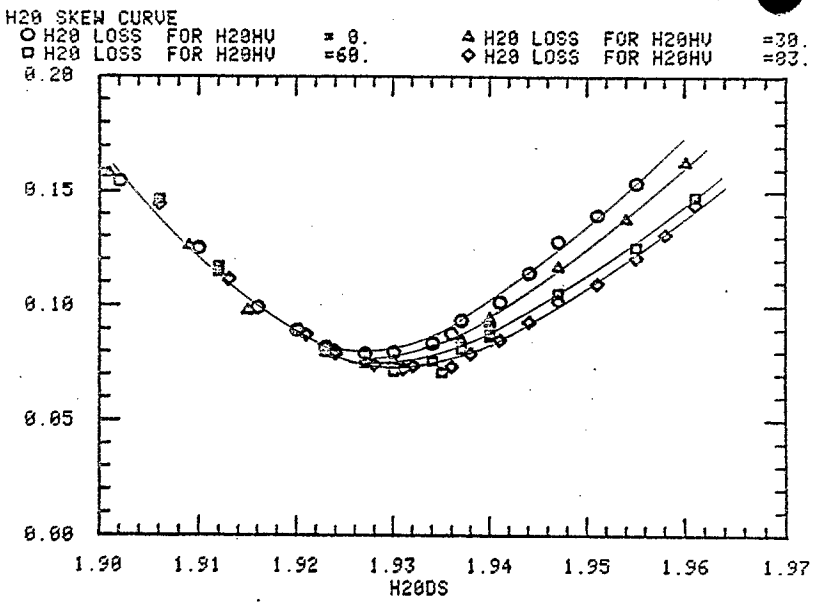

Fig. 21 Loss at H20 vs H20 septum skew, at four different applied voltages. The horizontal axis gives the radial position in inches of the septum extrapolated to a point 84.5 inches downstream of the leading edge. A point on the septum 1.5 inches downstream of the leading edge was held fixed. Measurements were made with the spiral pitch at F5 equal to 0.6 inches.

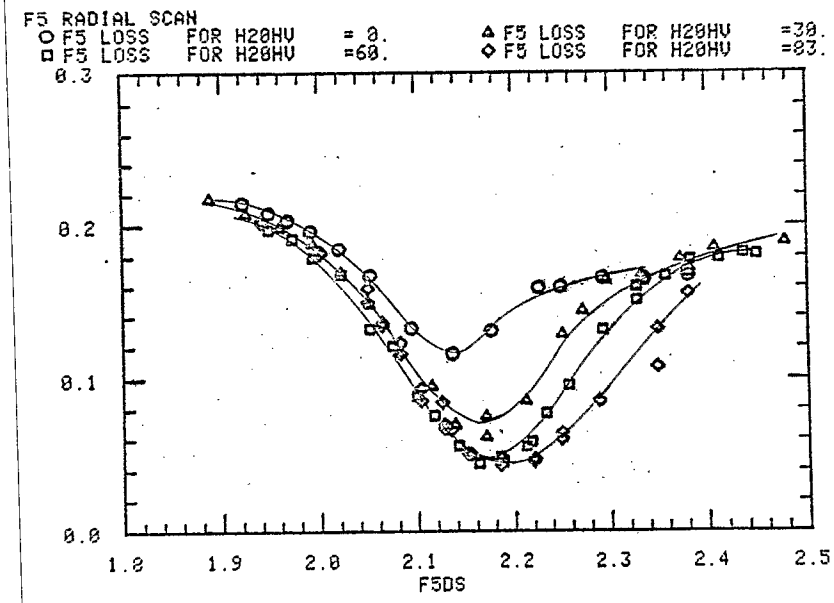

Fig. 22 Loss at F5 vs F5 radial position (inches). The skew angle was held constant. The spiral pitch at F5 was 0.6 inches.